THE JOURNAL OF PHYSICAL CHEMISTRY A
A JOURNAL OF THE AMERICAN CHEMICAL SOCIETY

pubs.acs.org/JPCA

Article

Extraction of Weak Spectroscopic Signals with High Fidelity: Examples from ESR

Madhur Srivastava,* Boris Dzikovski, and Jack H. Freed*

Cite This: *J. Phys. Chem. A* 2021, 125, 4480–4487

Read Online

ACCESS | Metrics & More | Article Recommendations | Supporting Information

ABSTRACT: Noise impedes experimental studies by reducing signal resolution and/or suppressing weak signals. Signal averaging and filtering are the primary methods used to reduce noise, but they have limited effectiveness and lack capabilities to recover signals at low signal-to-noise ratios (SNRs). We utilize a wavelet transform-based approach to effectively remove noise from spectroscopic data. The wavelet denoising method we use is a significant improvement on standard wavelet denoising approaches. We demonstrate its power in extracting signals from noisy spectra on a variety of signal types ranging from hyperfine lines to overlapped peaks to weak peaks overlaid on strong ones, drawn from electron-spin-resonance spectroscopy. The results show that one can accurately extract details of complex spectra, including retrieval of very weak ones. It accurately recovers signals at an SNR of ∼1 and improves the SNR by about 3 orders of magnitude with high fidelity. Our examples show that one is now able to address weaker SNR signals much better than by previous methods. This new wavelet approach can be successfully applied to other spectroscopic signals.

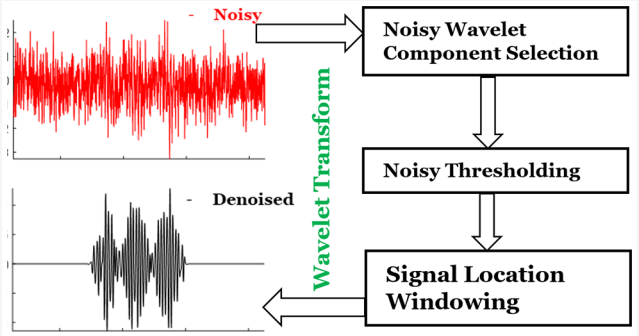

INTRODUCTION

Studies in spectroscopy rely on the quality of the data for accurate analysis. However, the presence of noise in experiments limits the findings, especially when the signals are very weak. In many cases, the experiments fail to produce a high quality signal despite extensive signal averaging, the standard method to reduce noise. Many postprocessing noise filtering methods have been used in spectroscopy,[1−8] but they are mainly effective for higher signal-to-noise ratios (SNRs) (SNR > 30). Wavelet transform (WT)-based denoising methods can reliably distinguish noise and signal in the wavelet domain, but the standard wavelet denoising methods[9−11] and their application in spectroscopic signals[3−8] have had limited success, and one desires to achieve wavelet denoising's true potential, particularly at low SNRs.

To denoise weaker signals, for example, at SNRs of ∼1, we utilize, in this work, new features in wavelet denoising methods that enable better separation of noise and signals in the wavelet domain. Key features and their effectiveness are described in prior work[12−15] that include (1) better signal and noise resolution in the wavelet domain and (2) improved noise thresholding. In this work, we add a new feature (3) signal identification in the wavelet domain,[16] and we show with this new feature that signal recovery is further improved by separating the noise and signal coefficients in wavelet domain, when both of them have comparable magnitude. We use examples from continuous wave ESR (cw-ESR), demonstrating how this improved method retrieves signal from noise, including from very weak signals and overlapping ones. We show that the signal resolution is greatly improved with as much as 3 orders-of-magnitude increase in the SNR and with high fidelity. With the ability to accurately retrieve signals at an SNR of ∼1:

1. Fewer scans are needed to recover the signal, so the signal acquisition time can be greatly reduced.
2. Both strong and weak signals in the spectra can simultaneously be recovered.
3. Fine features, such as superhyperfine lines, can be reliably distinguished.

The method is general and can be applied to any magnetic resonance and molecular spectroscopic or other data.

METHODS

Wavelet Transforms. A signal can be analyzed in the signal domain (such as time and space, among others) where it is acquired or a transformed domain in which some characteristics/features of a signal are especially prominent.[17] The Fourier transform (FT) is the most common as it provides frequency information for the complete signal. However, the FT

Received: March 12, 2021
Revised: May 4, 2021
Published: May 19, 2021

https://doi.org/10.1021/acs.jpca.1c02241
J. Phys. Chem. A 2021, 125, 4480–4487

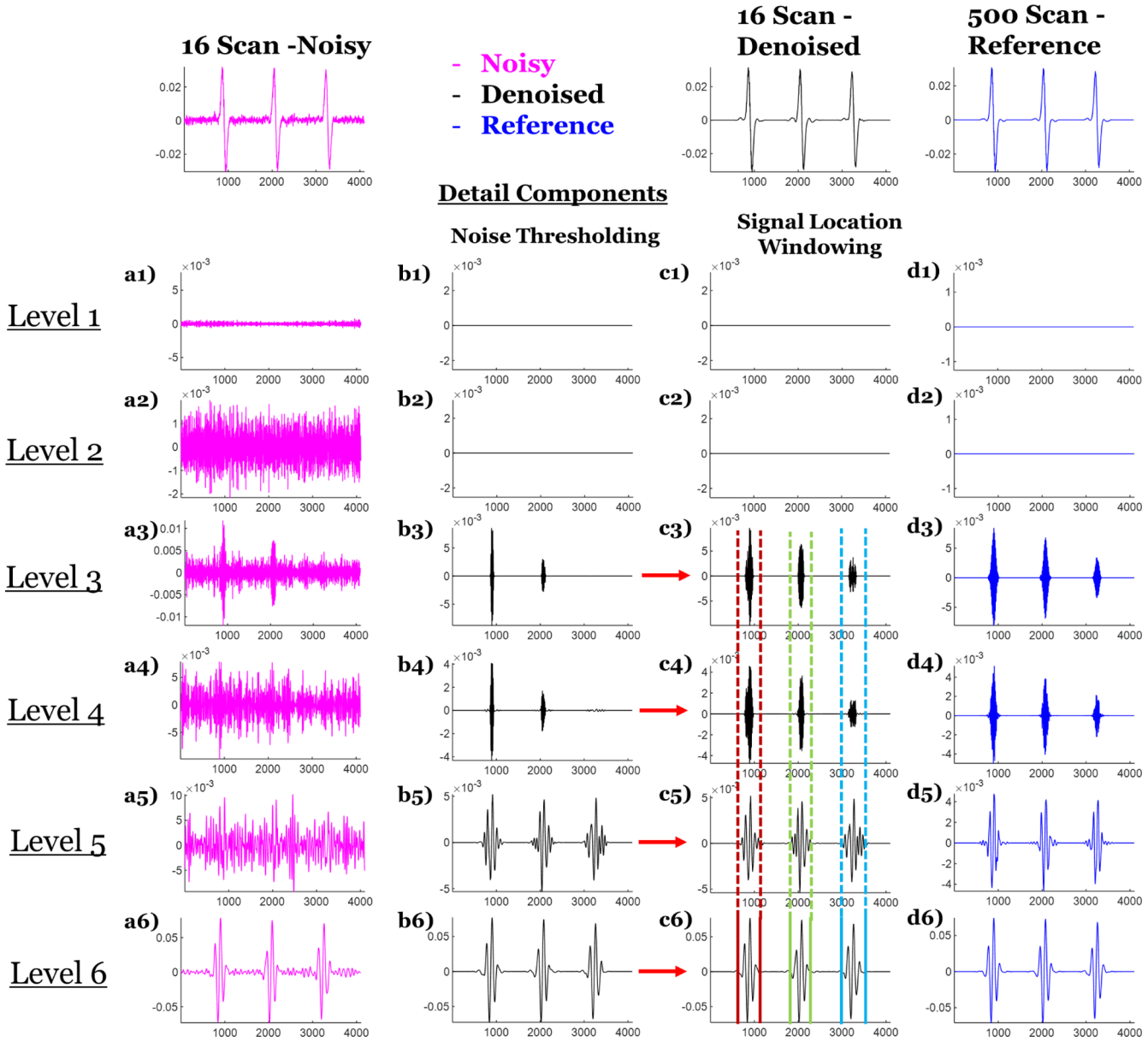

Figure 1. Example showing the denoising procedure. (a1−a6) Original decomposition level components and prior to noise thresholding; (b1−b6) levels after the noise thresholding procedure; (c1−c6) levels after signal location windowing based on (b6); (d1−d6) same decomposition levels obtained from the reference signal. As noted, (b6) is used to locate the windows. After windowing (c3,c4) are rendered in good agreement with reference (d3,d4), while even (c5) is slightly improved. Note that the windowing is not applied to (c1,c2) because they are all noise as can be seen from (d1,d2).

cannot provide frequency information for a "localized" signal region (e.g., time) nor does it show how frequency information is changing from the start of the signal to its end. WTs can provide these types of information. Furthermore, in a WT, we can localize the signal and frequency information from single data points to the complete signal. WTs also display local signal features when observed from a frequency sub band. This allows comprehensive analysis of a signal. Mathematically, a WT is defined as[14,18]

$$F(\tau, s) = \frac{1}{\sqrt{|s|}} \int_{-\infty}^{+\infty} f(t)\psi^*\left(\frac{t-\tau}{s}\right)\mathrm{d}t \quad (1)$$

where s is the inverse frequency (or frequency range) parameter, τ is the signal localization parameter, t represents the signal location, $f(t)$ is the signal, $F(\tau, s)$ is the wavelet-transformed signal at a given signal localization and frequency, and $\psi^*\left(\frac{t-\tau}{s}\right)$ is the signal probing function called "wavelet." Different wavelets are used to vary selectivity or sensitivity of adjacent frequencies with respect to signal localization. They are not dependent on a priori information of the signal or its characteristics. Depending on the application, different wavelets can be selected.

Like the FT, a WT has high computational complexity, and hence, for practical implementation, the discrete WT (DWT) is used. To avoid redundancy and reduce computational complexity, WTs are taken over nonoverlapping frequency ranges called "sub bands" or "detail components" in wavelet terminology. To differentiate between different detail components, sub bands containing the highest frequencies are called the "detail component at decomposition level 1" and sub bands containing

https://doi.org/10.1021/acs.jpca.1c02241
J. Phys. Chem. A 2021, 125, 4480−4487

lower frequencies are labeled in the ascending numerical order of the decomposition level. At each decomposition level, the residual lower frequency sub band is stored as the "approximation component" at that decomposition level so that signal information at all the frequencies is still contained at any given decomposition level.

Wavelet Denoising. The word "denoising" to remove noise was first used in the context of WTs.[10] Unlike FT and short time FT (STFT), the WT can identify and distinguish noise and signal frequencies using the signal domain-frequency representation that is reflected through the approximation and detail components and their decomposition levels. The separation of noise from signal in WT relies on the following:

1. Noise and signal will typically not have the same frequency at the same signal location because all the noise frequencies do not occur at every signal location. Therefore, when noise and signal frequencies overlap in the approximation and detail components, they can be distinguished using the signal location information.
2. For rare cases where noise and signals have the same frequency at the same signal location, the noise strength at that location is usually negligible compared to the signal strength or the contribution of the information in the overall signal is minuscule.
3. The signal strength is substantially greater than the noise strength in the wavelet domain. This is because the signal is coherent and is represented by a few wavelet coefficients with high magnitude. In contrast, noise, being random, is represented by many coefficients each with small magnitude. It is based on the entropy concept: randomness has higher entropy.

Noise Elimination and Reduction via Denoising (NERD). The methodology is described in detail in the Supporting Information. However, we illustrate the method in Figure 1. The average of a 16-scan noisy ESR signal from a nitroxide is shown in the upper left, which is collected in 4096 points. It is transformed into the discrete wavelet domain as shown in subfigures labeled a. Here, level 1 is the highest frequency band, with each successive level representing a lower frequency band. The x-axis corresponds to 4096 discrete points in the signal localization parameter, τ (cf. eq 1). The higher frequency levels are largely noise, whereas the lowest levels are mostly signals. After the denoising process, also known as noise thresholding, only signal components remain as shown in subfigures labeled b. However this procedure, which eliminates the noise coefficients that are weak in the wavelet domain (cf. comment #3 above), also removes signal coefficients whose magnitude is less than the maximum magnitude of noise coefficients. This is a weakness of all previous methods including our original one.[12,14] To overcome this weakness, we introduce the new concept of signal location windowing.[16] In this step, illustrated in subfigures labeled c, the vertical lines in purple, green, and blue delineate the "windows". They are determined from subfigure b6 that clearly shows the dominant signal regions, which must contain some semblance of the signal in the higher frequency levels 3, 4, and 5. Thus, within these three windows, one restores the components that had been eliminated by the prior noise thresholding step. Levels 1 and 2 are not included in this step because they are dominated by high frequency noise. Finally, one may compare the "windowed" results in subfigures c with the wavelet components shown in subfigures d that are obtained from the virtually noise-free average of a 500 scan reference spectrum shown in the upper right corner of Figure 1. One sees significantly better agreement between the "windowed" components in subfigures c and the reference results in subfigure d than is the case for the components in subfigures b. The results in subfigures c are then converted back into the original ESR signal by inverse transformation (see the Supporting Information section Wavelet Denoising), which now has had its noise removed, that is, it is "denoised". In the next section, we show with examples from several types of ESR cases the power of this method, which we call noise elimination and reduction or NERD. As noted above, a more detailed description of NERD is given in the Supporting Information.

Denoising ESR Spectra. We use cw-ESR spectroscopy data for testing and demonstrating the effectiveness of NERD. cw-ESR is used extensively to study the dynamics and structure of biomolecules and is the most commonly used ESR technique.[19] The cw-ESR spectrum is acquired in the magnetic field (B_0) domain, which is swept, that is, $B_0 = B_0(t)$ in a linear fashion. Moreover, a variety of spectra can be provided as test signals.

ESR Experiment and Sample Preparation. We acquired three types of experimental signals as examples showing the power of the denoising method. Example 1 contains three main ^{14}N components and six weak ^{13}C ones. The sample used was a 50 μM aqueous solution of Tempol (4-hydroxy-2,2,6,6-tetramethylpiperidine 1-oxyl).[19−22] The ESR experiments were performed at 20 °C on a commercial spectrometer (Bruker ELEXYS-II E500) at 9.4 GHz microwave frequency that corresponds to a 0.34 T dc magnetic field. The spectral data set consisted of 4096 points along the magnetic field sweep. It provides both strong and weak spectral features for denoising.

Example 2 provides a more overlapped signal to study. The sample consisted of a concentrated water suspension of multilamellar vesicles of DMPC (1,2-dimyristoyl-*sn*-glycero-3-phosphocholine) doped with 0.5% of a lipid spin label, 16-PC (1-acyl-2-[16-(4,4-dimethyloxazolidine-*N*-oxyl)stearoyl]-*sn*-glycero-3-phosphocholine). The spectra were recorded in the liquid crystalline membrane (L^{β}) phase at 37 °C on a home-built ACERT 95 GHz ESR spectrometer[21] with a dc magnetic field of 3.3 T. The spectral data set contained 512 data points.

Example 3 contains multiple narrow ESR lines due to the interaction of the unpaired electron with a ^{14}N nucleus and several protons. The radical di-(4-*tert*-butyl-phenyl) nitroxide was dissolved in toluene at a 100 μM concentration and thoroughly deoxygenated using the freeze-thaw technique. The spectra were recorded under the same conditions as for sample 1. However, a small magnetic field modulation at 100 kHz of 20 mG was used to produce the weak signal obtained from a single scan, whereas the strong reference signal from an average of 500 scans was obtained with a 100 mG field modulation to enhance the signal and suppress noise. (Magnetic field modulation is used to provide the derivative of the absorption signal.[19])

Signal Averaging. In example 1, two separately averaged signals were generated by averaging 4 and 16 scans, resulting in SNRs of 15 and 57, respectively, for the main components and SNRs of 1.5 and 0.5, respectively, for the weak components (cf. Table 1). A reference signal was also generated by averaging 500 scans. In example 2, three noisy signals were generated by averaging 1, 4, and 18 scans. Their respective SNRs were 10, 19, and 39. Example 3 is noted in the previous paragraph.

Objective Measures. *Signal-to-Noise Ratio (SNR).* To test the efficacy of NERD, the SNR is used for calculating the noise

https://doi.org/10.1021/acs.jpca.1c02241
J. Phys. Chem. A 2021, 125, 4480−4487

Table 1. Example 1—SNR and SSIM of Noisy and Denoised Signals at 16- and 4-Scan

data averaging		noisy SNR	noisy SSIM	denoised SNR	denoised SSIM
16-scan	signal	57	0.9899	9.2×10^4	0.9975
	peak 1	0.5	0.1885	2.1×10^3	0.8244
	peak 2	15	0.9967	4.6×10^4	0.9976
	peak 3	10	0.9925	4.6×10^4	0.9942
	peak 4	0.7	0.1027	2×10^3	0.8329
	peak 5	0.7	0.2018	1.9×10^3	0.7274
	peak 6	14	0.9970	4.4×10^4	0.9975
	peak 7	14	0.9962	4.4×10^4	0.9974
	peak 8	0.9	0.1980	2×10^3	0.6149
	peak 9	1.1	0.3249	1.5×10^3	0.9267
	peak 10	19	0.9985	4.3×10^4	0.9987
	peak 11	20	0.9985	4.2×10^4	0.9988
	peak 12	0.3	0.0811	322	0.5439
4-scan	signal	15	0.9724	4.7×10^3	0.9992
	peak 1	0.3	0.0067	NA-distorted	0.1201
	peak 2	9	0.9931	2.4×10^3	0.9974
	peak 3	8	0.9896	2.2×10^3	0.9936
	peak 4	0.3	−0.0264	NA-distorted	0.1949
	peak 5	0.3	0.0133	179	0.6668
	peak 6	10	0.9939	2.3×10^3	0.9985
	peak 7	7	0.9866	2.3×10^3	0.9940
	peak 8	0.4	0.0393	NA-distorted	0.2034
	peak 9	0.4	0.1077	192	0.8161
	peak 10	8	0.9923	2.3×10^3	0.9968
	peak 11	7	0.9904	2.1×10^3	0.9934
	peak 12	0.4	0.0565	126	0.7855

presence in the noisy and denoised signals. The SNR is defined as

$$\mathrm{SNR} = \frac{\mathrm{signal}_{\mathrm{peak}}}{\mathrm{noise}_{\mathrm{rms}}} \tag{2}$$

where $\mathrm{signal}_{\mathrm{peak}}$ is the maximum peak height of the signal and $\mathrm{noise}_{\mathrm{rms}}$ is the root-mean-square of the noise present. The noise present is measured from spectral positions where there is no signal present in the experimental data. The SNR is thus the inverse of the amount of noise present with respect to the maximum peak height of the signal. Of course, the remaining signal peaks, whose maxima are less than the maximum peak height, have lower SNRs.

We also use $\mathrm{SNR}_{\mathrm{peak\text{-}to\text{-}peak}}$ to calculate the SNR of the overall signal as follows

$$\mathrm{SNR}_{\mathrm{peak\text{-}to\text{-}peak}} = \frac{\mathrm{signal}_{\mathrm{peak\text{-}to\text{-}peak}}}{\mathrm{noise}_{\mathrm{rms}}} \tag{3}$$

where $\mathrm{SNR}_{\mathrm{peak\text{-}to\text{-}peak}}$ is the magnitude between maximum and minimum peak heights.

Equations 2 and 3 are used for calculating local and global SNRs, respectively. Since signals shown in the examples contain multiple peaks with different magnitudes, eq 2 is used to find the SNR of each peak. Equation 3, on the other hand, provides the standard measure of the overall SNR for the complete signal, which is composed of derivatives of the absorption.

Structural Similarity Index Measure (SSIM). Although the SNR provides noise error bounds and confidence measures for the recovered signal, it lacks information on how well the signal is recovered, that is, its fidelity. We use the structural similarity

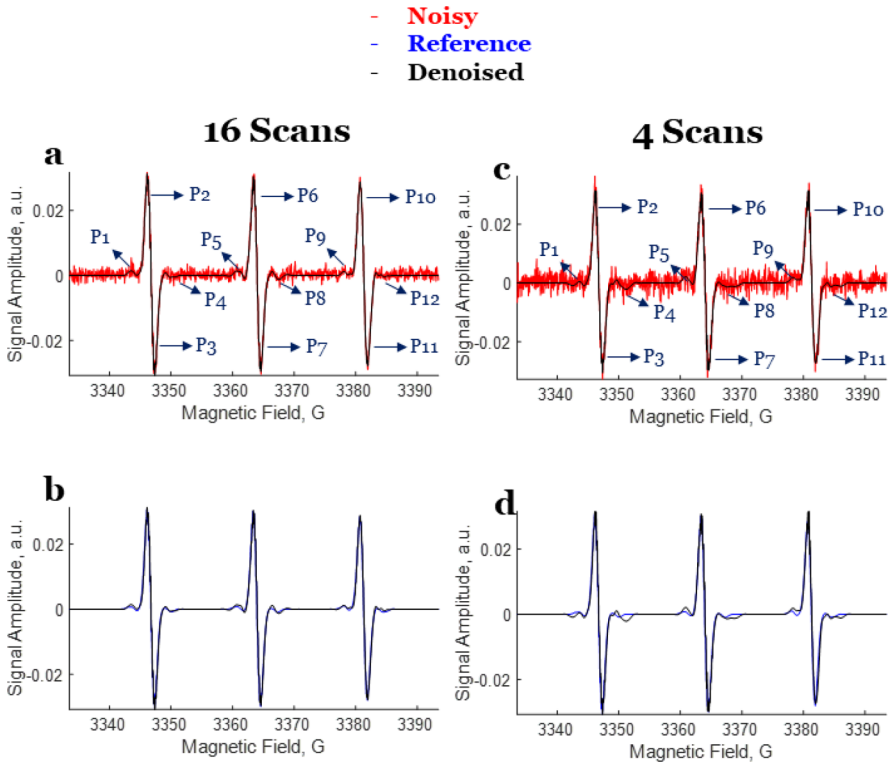

Figure 2. Experimental data example 1—results of NERD at 16- and 4-scan cw-ESR spectra with the SNR at individual peaks in Table 1. (a) 16-scan noisy signal overlapped with its denoised signal, (b) denoised signal of the 16-scan noisy signal overlapped with the reference signal, (c) 4-scan noisy signal overlapped with its denoised signal, and (d) denoised signal of the 4-scan noisy signal overlapped with the reference signal. P1 is peak 1.

https://doi.org/10.1021/acs.jpca.1c02241
J. Phys. Chem. A 2021, 125, 4480−4487

index measure (SSIM)[23] to complement the SNR as the criterion for the signal recovery. The SSIM can be calculated as

$$\mathrm{SSIM}(X, Y) = \frac{(2\mu_X\mu_Y + c_1)(2\sigma_{XY} + c_2)}{(\mu_X^2 + \mu_Y^2 + c_1)(\sigma_X^2 + \sigma_Y^2 + c_2)} \quad (4)$$

where X is the noisy or denoised signal; Y is the reference signal; μ_X and μ_Y are the mean values of X and Y, respectively; σ_X and σ_Y are the standard deviations of X and Y, respectively; σ_{XY} is the covariance of X and Y; and c_1 and c_2 are small positive constants used for stabilizing each term. The range $[-1, 1]$ reflects the resemblance of X w.r.t. Y. For identical X and Y, the SSIM is 1. In all the examples described in the next section, the experimental result to be used as the reference signal was first denoised to remove the small amount of residual noise to better serve as the reference.

In addition to finding the SSIM of the complete signal, we also obtained localized SSIMs for individual peak regions. Because the strong peaks can overwhelm or dominate the overall SSIM value, the local SSIM provides better information about the fidelity of each peak for noisy and denoised data. To ensure the appropriate measure, c_1 and c_2 were selected to be 10% of the peak magnitude of the peak under consideration.

Software Availability. The NERD method is available both in automated and user interface forms. The website denoising.cornell.edu contains all the steps required for denoising, including wavelet selection, decomposition level selection, noise thresholding, and signal location windowing. The automated code for each step is continuously added to the online software and can also be requested from the authors. The process to develop the automated code is provided in our patent and publications.[12−16] The user interface, in addition to denoising, can be used to overcome anomalies in experimental data such as those associated with artifacts.

RESULTS AND DISCUSSION

Example 1: Nonoverlapping Signals with the Superhyperfine Structure. The results of example 1 are shown in Figures 2 and 3 and Table 1. (The numbering of the peaks is given in Figure 2a,c.) Note that peaks 2, 3, 6, 7, 10, and 11 are the strong peaks from ^{14}N hyperfine splitting (hfs) and peaks 1, 4, 5, 8, 9, and 12 are the weak (hfs) peaks from ^{13}C in natural abundance (1.1%). The strong peaks, with overall SNRs of 57 for the 16-scan average and 15 for 4-scan, are well recovered before and after denoising. The weak peaks are not observable in the original "noisy" spectra in either case of signal averaging. However, Figure 2b shows that they are recovered for the 16-scan cases, but only partially for the 4-scan case (Figure 2d). The noisy SNRs and the SSIMs for both the noisy and denoised weak peaks are given in Table 1.

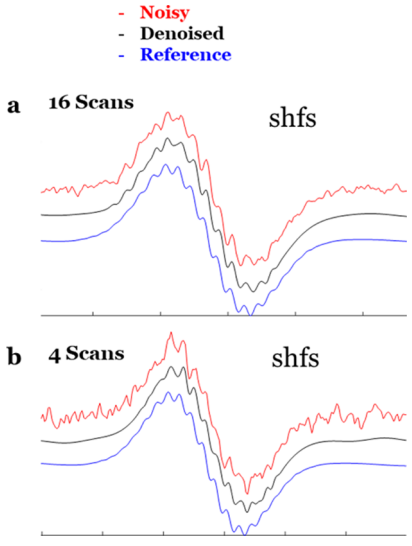

Figure 3. Experimental data example 1—results of the strong peak obtained from the NERD method at 16-scan (a) and 4-scan (b) showing shfs. NERD denoised signals are compared with the reference and noisy signals.

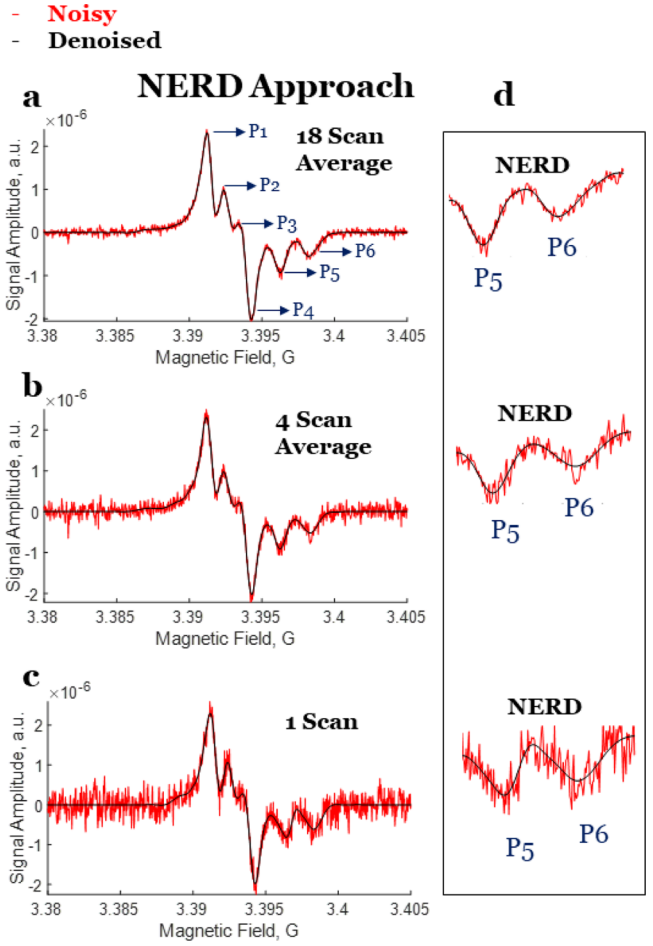

Figure 4. Experimental data example 2—results of NERD at 18-, 4-, and 1-scan cw-ESR data with the SNR in Table 2. (a) 18-scan noisy signal overlapped with NERD denoised data, (b) 4-scan noisy signal overlapped with NERD denoised data, (c) 1-scan noisy signal overlapped with NERD denoised data, and (d) peaks 5 and 6 are blown up showing great fidelity with NERD especially for the 1-scan case.

We first consider the 16-scan case. The original SNR for the weak peaks is around unity ($\gtrsim$0.5), but very good to excellent recovery is achieved for most of them. In the 4-scan case, the weak peaks have noisy SNRs <0.5 (generally about half that for the 16-scan case, as expected), implying that there is still a substantial noise presence in the designated signal coefficients we are retaining. NERD does however inform about the accurate peak locations. In summary, these results do indicate that when the initial SNR $\gtrsim$0.5, NERD is reliable in recovering the signal.

There is another feature of these spectra to test the method. When the main peaks are spread out as in Figure 3a,b, one observes the superhyperfine structure (shfs) on them due to ^{1}H

https://doi.org/10.1021/acs.jpca.1c02241
J. Phys. Chem. A 2021, 125, 4480−4487

Table 2. Example 2—SNR and SSIM of Noisy and Denoised Signals[a]

data averaging		SNR		SSIM	
		noisy	NERD	noisy	NERD
18-scan	signal	73	1.1×10^8	NA	NA
	peak 1	38	6.1×10^7	NA	NA
	peak 2	17	2.5×10^7	NA	NA
	peak 3	2.7	5.1×10^6	NA	NA
	peak 4	32	5.3×10^7	NA	NA
	peak 5	13	2.4×10^7	NA	NA
	peak 6	9	1.4×10^7	NA	NA
4-scan	signal	33	1.1×10^5	0.8830	0.9968
	peak 1	17	6.04×10^4	0.9073	0.9934
	peak 2	8	2.5×10^4	0.9269	0.9899
	peak 3	3	5.8×10^3	0.8741	0.9753
	peak 4	14	5.3×10^4	0.9208	0.9964
	peak 5	7	2.4×10^4	0.9182	0.9982
	peak 6	6	1.3×10^4	0.8971	0.9945
1-scan	signal	21	3.2×10^4	0.6938	0.9946
	peak 1	9	1.7×10^4	0.7684	0.9978
	peak 2	4	8.1×10^3	0.7324	0.9804
	peak 3	2	2.1×10^3	0.6554	0.9391
	peak 4	9	1.5×10^4	0.8018	0.9935
	peak 5	4	5.7×10^3	0.7827	0.9866
	peak 6	5	4.6×10^3	0.6823	0.9895

[a]SNR is calculated at 18-, 4-, and 1-scan at different peaks, whereas SSIM is obtained for 4- and 1-scan because denoised NERD data at 18-scan are used as the reference. Hence, not applicable (NA) is noted for 18-scan SSIM values for noisy and denoised data. SSIM constant parameters are selected as $c_1 = c_1 = 10^{-13}$ in order to measure the small differences in the spectrum. Signal refers to the complete spectrum for which the SNR and SSIM are obtained, and peak refers to SNR and SSIM values for individual peak regions.

hf lines. We see in Figure 3a, for the 16-scan case, the excellent recovery of this shfs, whereas in the original noisy spectrum, it is somewhat corrupted. For the 4-scan case, NERD is still successful (cf. Figure 3b), whereas it is substantially corrupted in the noisy spectrum. The importance of signal location windowing here is that it retains the shfs and just removes the noise. In the absence of windowing, the shfs is also largely suppressed by denoising, especially in the 4-scan case.

Example 2: Overlapped Signals. In example 2 shown in Figure 4, NERD is applied to 18-scan, 4-scan, and 1-scan signal-averaged noisy data. The overall signal SNRs for each of them are 73, 33, and 21, respectively, and the minimum peak SNR is 2 (with an SSIM value of 0.6554) for peak 3 of the 1-scan case. As with the previous experimental case, one can see that the denoised results enhance the SNR for each peak and the overall signal SNR by several orders of magnitude for 18-, 4-, and 1-scan (cf. Table 2). More importantly, the denoised signal is able to successfully extract the lineshapes that are buried under the noise. For example, the third peak in subfigure c is overwhelmed by noise with little evidence of its presence. After denoising, this peak is now well resolved as we see by comparing with the 18-scan denoised spectra.

Example 3: Hyperfine Spectra. Example 3 demonstrates the ability of NERD to extract a periodic, repeating pattern in the processed data from a signal with an SNR of ∼unity (cf. Figure 5a). The reference spectrum of di-(4-*tert*-butyl-phenyl) nitroxide in degassed toluene is shown in Figure 5c obtained from 500 averages and more favorable experimental conditions. It

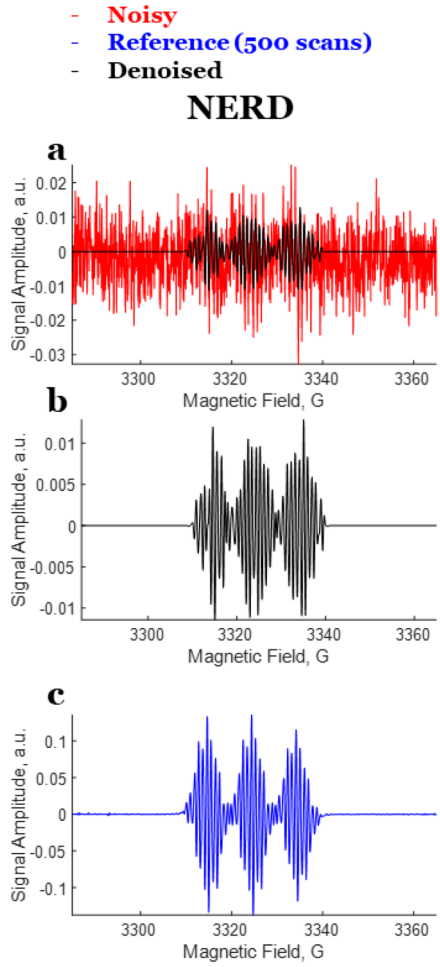

Figure 5. Experimental data example 3—results of the NERD for a cw-ESR hyperfine data set with an SNR of ∼1. (a) NERD denoised signal superposed on the original noisy signal, (b) NERD denoised data, and (c) reference data. The reference data were acquired with 500 scans at higher modulation amplitude.

Table 3. Example 3—SNR and SSIM of Noisy and Denoised Signals[a]

	noisy	NERD	reference
SNR	1.1	8.5×10^3	1.7×10^4
SSIM	0.08	0.9608	NA
hyperfine lines	NA	66	66

[a]The table also shows the number of hyperfine lines retrieved by the NERD method. The SNR for the reference was obtained under different experimental conditions to guarantee a very high SNR.

consists of many narrow hf lines. This hyperfine structure is from three main groups of lines due to the ^{14}N nucleus; each of these is further split into a larger number of lines resulting from the interaction of the unpaired electron with two groups of four equivalent protons in the ortho- and meta-positions relative to the nitroxide moiety, that is, four ortho protons split each ^{14}N hf line into a quintet of hf lines, and each of them is further split into a quintet of hf lines by the four meta protons. These hf lines overlap, so the whole spectrum is difficult to analyze or even detect in the presence of substantial noise. However, NERD has the unique ability to elicit the periodic patterns that are undetectable by the eye. It is able to recover all 66 peaks with high fidelity (SNR = 8.5×10^3 and SSIM = 0.9608, cf. Table 3)

https://doi.org/10.1021/acs.jpca.1c02241
J. Phys. Chem. A 2021, 125, 4480−4487

from an initial noisy spectrum SNR of 1.1 and SSIM value of 0.08. The hyperfine lines appear in distinct positions, represented by a few wavelet coefficients, and can be readily separated by NERD from the random noise (cf. Figure 5a,b). The NERD result compares very favorably with the reference (cf. Figure 5c), providing nearly perfect recovery of all features. In the absence of signal location windowing, most of the hyperfine lines cannot be recovered.

CONCLUSIONS

In this paper, we have shown that the NERD method significantly enhances the denoising capabilities so that weak signals with SNRs on the order of unity can be recovered with high fidelity and of the order of 3 orders of magnitude increase in SNR. This capability of recovering weak signals represents a significant improvement over previous wavelet denoising methods. We have supplied three distinct examples in this paper from ESR spectroscopy (out of numerous others) that demonstrate in several ways the great power of NERD in recovering spectral details even from cases where they appear to be buried within the noise. This can allow studies to be conducted at low sample concentrations and/or studies that were not feasible due to long acquisition times, given that using NERD reduces required signal averaging times by orders of magnitude. Since NERD requires no prior information about the signal nor is tailored for any particular type of signal, it can be used to recover weak signals obtained in many fields of study. In addition, it can be adapted to two-dimensional spectroscopy.[12−16,18]

ASSOCIATED CONTENT

Supporting Information

The Supporting Information is available free of charge at https://pubs.acs.org/doi/10.1021/acs.jpca.1c02241.

NERD algorithm; discrete WT: background and mathematical formulation; and wavelet denoising: process and formulae, including figures (PDF)

AUTHOR INFORMATION

Corresponding Authors

Madhur Srivastava − *Department of Chemistry and Chemical Biology, Cornell University, Ithaca 14853, United States; National Biomedical Center for Advanced Electron Spin Resonance Technology, Cornell University, Ithaca 14853, United States;* orcid.org/0000-0002-2095-0412; Email: ms2736@cornell.edu

Jack H. Freed − *Department of Chemistry and Chemical Biology, Cornell University, Ithaca 14853, United States; National Biomedical Center for Advanced Electron Spin Resonance Technology, Cornell University, Ithaca 14853, United States;* orcid.org/0000-0003-4288-2585; Email: jhf3@cornell.edu

Author

Boris Dzikovski − *Department of Chemistry and Chemical Biology, Cornell University, Ithaca 14853, United States;* Present Address: Bruker BioSpin Corp., Billerica 01821, USA.; orcid.org/0000-0002-5687-5207

Complete contact information is available at: https://pubs.acs.org/10.1021/acs.jpca.1c02241

Notes

The authors declare no competing financial interest.

The NERD software can be accessed through denoising.cornell.edu. The reader is encouraged to reach out to the authors for more information.

ACKNOWLEDGMENTS

The authors would like to thank Prof. V. Livshits for providing the radical di-(4-*tert*-butyl-phenyl) nitroxide. This work was supported by the National Institute of General Medical Sciences/National Institutes of Health under grant P41GM103521.

REFERENCES

(1) Kusaka, Y.; Hasegawa, T.; Kaji, H. Noise Reduction in Solid-State NMR Spectra Using Principal Component Analysis. *J. Phys. Chem. A* **2019**, *123*, 10333−10338.

(2) Hu, Y.; Li, B.; Sato, H.; Noda, I.; Ozaki, Y. Noise Perturbation in Functional Principal Component Analysis Filtering for Two-Dimensional Correlation Spectroscopy: Its Theory and Application to Infrared Spectra of a Poly(3-hydroxybutyrate) Thin Film. *J. Phys. Chem. A* **2006**, *110*, 11279−11290.

(3) Taylor, J. N.; Landes, C. F. Improved Resolution of Complex Single-Molecule FRET Systems via Wavelet Shrinkage. *J. Phys. Chem. B* **2011**, *115*, 1105−1114.

(4) Taylor, J. N.; Makarov, D. E.; Landes, C. F. Denoising Single-Molecule FRET Trajectories with Wavelets and Bayesian Inference. *Biophys. J.* **2010**, *98*, 164−173.

(5) Barclay, V. J.; Bonner, R. F.; Hamilton, I. P. Application of Wavelet Transforms to Experimental Spectra: Smoothing, Denoising, and Data Set Compression. *Anal. Chem.* **1997**, *69*, 78−90.

(6) Chen, H.; Xu, W.; Broderick, N.; Han, J. An adaptive denoising method for Raman spectroscopy based on lifting wavelet transform. *J. Raman Spectrosc.* **2018**, *49*, 1529−1539.

(7) Ehrentreich, F.; Sümmchen, L. Spike Removal and Denoising of Raman Spectra by Wavelet Transform Methods. *Anal. Chem.* **2001**, *73*, 4364−4373.

(8) Shao, X.-G.; Leung, A. K.-M.; Chau, F.-T. Wavelet: A New Trend in Chemistry. *Acc. Chem. Res.* **2003**, *36*, 276−283.

(9) Fodor, I. K.; Kamath, C. Denoising through wavelet shrinkage: an empirical study. *J. Electron. Imag.* **2003**, *12*, 151−160.

(10) Donoho, D. L. De-noising by soft-thresholding. *IEEE Trans. Inf. Theory* **1995**, *41*, 613−627.

(11) Donoho, D. L.; Johnstone, I. M. Ideal Spatial Adaptation by Wavelet Shrinkage. *Biometrika* **1994**, *81*, 425−455.

(12) Srivastava, M.; Anderson, C. L.; Freed, J. H. A New Wavelet Denoising Method for Selecting Decomposition Levels and Noise Thresholds. *IEEE Access* **2016**, *4*, 3862−3877.

(13) Srivastava, M.; Georgieva, E. R.; Freed, J. H. A New Wavelet Denoising Method for Experimental Time-Domain Signals: Pulsed Dipolar Electron Spin Resonance. *J. Phys. Chem. A* **2017**, *121*, 2452−2465.

(14) Srivastava, M. Improving Signal Resolution and Reducing Experiment Time in Electron Spin Resonance Spectroscopy via Data Processing Methods. Ph.D. Thesis, Cornell University, 2018.

(15) Srivastava, M.; Anderson, C. L.; Freed, J. H. Systems, Methods and Programs for Denoising Signals using Wavelets. U.S. Patent 20,190,287,220 A1, 2021.

(16) Srivastava, M.; Freed, J. H. Wavelet denoising using signal location windowing. U.S. Patent 63/043,447, 2020.

(17) Daubechies, I. *Ten Lectures on Wavelets*, 1st ed.; SIAM: Philadelphia, Pennsylvania, 1992.

(18) Addison, P. *The Illustrated Wavelet Transform Handbook: Introductory Theory and Applications in Science, Engineering, Medicine and Finance*, 2nd ed.; CRC Press: London, U.K., 2016.

(19) Weil, J. A.; Bolton, J. R. *Electron Paramagnetic Resonance: Elementary Theory and Practical Applications*; John Wiley & Sons, Ltd: Hoboken, New Jersey, 2006.
(20) Freed, J. H. New Technologies in Electron Spin Resonance. *Annu. Rev. Phys. Chem.* **2000**, *51*, 655−689.
(21) Hofbauer, W.; Earle, K. A.; Dunnam, C. R.; Moscicki, J. K.; Freed, J. H. High-power 95 GHz pulsed electron spin resonance spectrometer. *Rev. Sci. Instrum.* **2004**, *75*, 1194−1208.
(22) Freed, J. H. *Biomedical EPR, Part B: Methodology, Instrumentation, and Dynamics*; KluwerChapter ESR and Molecular Dynamics: New York, 2005; pp 239−268.
(23) Wang, Z.; Bovik, A. C.; Sheikh, H. R.; Simoncelli, E. P. Image quality assessment: from error visibility to structural similarity. *IEEE Trans. Image Process.* **2004**, *13*, 600−612.

https://doi.org/10.1021/acs.jpca.1c02241
J. Phys. Chem. A 2021, 125, 4480−4487